CHAPTER IV
HIGHLY CONDUCTIVE CARBON FOR APPLICATIONS IN SUPERCAPACITORS OR BATTERIES

4.1 Abstract

Supercapacitors are new kind of energy storage devices which have high efficiency and outstanding properties such as high power density and long life cycle. In order to reach high capacitance, choosing the electrode material is very important. Carbon materials are the great choice due to provide suitable properties for using as supercapacitor electrodes such as high electrical conductivity, flexible on morphology design, and low cost. Generally for high conductive carbon, graphene is a powerful candidate, but it has some drawbacks which are high production cost and difficult to process. Therefore synthesis of grapheme-like carbon is interested, in order to use as an alternative conductive material. In this study, sol-gel process was used to synthesize polybenzoxazine precursor, in which Cetyltrimethyl Ammonium Bromide (CTAB) was used as a soft template to produce amorphous carbon with high electrical conductivity. The chemical structure of polybenzoxazine was examined by FT-IR and TGA was used to investigate the thermal properties. In addition, the effect of pyrolysis temperature was investigated. The results showed that pyrolysis at 1000 ^{0}C provided the highest conductivity around 9800 S/cm because the structure of the resulting carbon changed to more ordered which observed from XRD pattern and Raman spectra. The electrical property of carbon xerogels were examined at room temperature by an electrometer with two-point probe.

Keywords: Polybenzoxazine, Sol-gel, Conductivity, Carbon

4.2 Introduction

Supercapacitors are new kinds of energy storage devices which divided into two types, electrical double layer capacitors and psuedocapacitors. Supercapacitors have various properties depends on electrode materials, types of electrolyte, and interfacial resistance between the electrode and current-collector [1]. Improving the performance of supercapacitors in order to compensate energy demand is realized. Choosing suitable electrode materials is the easiest way to improve the performance. Carbon materials are very attractive because of high electrical conductivity, high temperature stability, controllable pore structure, and acceptable cost. Focusing on carbon which has high electrical conductivity, graphene is outstanding.

Graphene is a two dimensional carbon sheet of sp^2-hybridized carbon. Normally single graphene layer is not a stable form and tend to restack themselves into 3D graphite through van der Waals interactions which lead to decreasing of electrical properties [2-3]. To overcome this interaction, many researchers try to prepare graphene via chemical process which including graphite oxidation, exfoliation, and reduction. Even through this process is easy to scale up but it consumed hazard chemicals and multi steps [4]. So in the present, preparation of graphene-like carbon structure from organic precursors is more attractive due to molecular design flexibility. In previous work, Worsley and coworker synthesized graphene aerogel via organic sol-gel and pyrolyzed at 1050 °C [5]. The results shown ultra-low-density three–dimensional graphene sheet and exposed high electrical conductivities ($1 \times 10^2\ S/m$). Choosing organic precursor which has high aromatic content can promote the electronic properties of the resulting carbon.

In traditional, carbon aerogel derived from resorcinol and formaldehyde due to desirable properties such as good mechanical strength, high dimensional stability but they also have some draw back such as poor shelf life, acid base catalyst required, and by-product released [6]. To eliminate the drawbacks, polybenzoxazine was developed and firstly synthesized by Holly and Cope which offer molecular design flexibility depends on precursors, no need strong acid base catalyst, and release of no by product [7]. Phenols, formaldehyde, and amines were used as starting materials for the synthesis of benzoxazine monomer. In order to reach the

goal that obtained high electrical conductivity carbon, carbon precursor with high aromatic contain and conjugated bonds was chosen because during the pyrolysis process at high temperature, carbons molecules would rearrange structure into higher order and lead to increasing of conductivity [8].

In the present work, polybenzoxazine was synthesized via sol-gel method to use as carbon precursor and then benzoxazine presursor was polymerized to become polybenzoxazine. After that polybenzoxazine was heat treated with various pyrolysis temperatures in order to study the changing of carbon structure which effect to electrical conductivity of carbon xerogels. The chemical composition of benzoxazine monomer composed of phenol, 4,4'-methylenedianiline (MDA), and formaldehyde. In addition, Hexadecyltrimethylammonium bromide (CTAB) also added to perform as surfactant in order to make the sol-gel structure looser. When the structure of polybenzoxazine looser which means that mobility of carbon structure during pyrolysis process was increased and created more chance for molecules to rearrange themselves into graphene-like structure during pyrolysis process.

4.3 Experimental

4.3.1 Materials

All chemicals were used without further purification. Polybenzoxazine precursor was synthesized using 4,4'-methylenedianiline (≥97%) was purchased from Fluka, Formaldehyde (37%wt. in water) was obtained from Merk Shap & Dohme Cooperation company and Phenol detached crystals (99.99%) was obtained from Fisher Chemical company. *N,N,* -dimethylformamide was used as solvent and purchased from RCI Labscan Co., Ltd. Hexadecyltrimethylammonium bromide (96%) was used as surfactant to expand the sol-gel structure obtained from Fluka Co., Ltd.

4.3.2 Measurements

The functional groups related to structure of materials were investigated by using FTIR technique. The FT-IR spectra were obtained using a Nicolet Nexus 670 FT-IR spectrometer in the frequency range of 400-4000 cm^{-1} with 64 scans at a resolution of 2 cm^{-1}. KBr pellet technique was applied in the

preparation of powder samples. DSC analyzer was carried out using a Perkin-Elmer DSC 7 instrument. The sample was heated from 25 to 300 °C with heating rate 10 °C per minute under N_2 atmosphere with flow rate 20 ml per minute. Finally, the heating profile, curing temperature and completely cured polybenzoxazine were obtained. TGA instrument was also conducted with Perkin Elmer Thermogravimetric /Differential Thermal Analyzer (TG-DTA). The sample was loaded in rang 4-8 mg on the alumina pan and heated from 50 to 900 °C under nitrogen atmosphere with flow rate 50 ml per minute and heating rate 10 °C per minute. The pyrolyzed temperature of polybenzoxazine was investigated from the onset temperature whereas char yield as the weight residue at 900 °C was reported. The X-ray powder diffraction pattern of the carbon foam was obtained using an XRD (Bruker AXS D8 ADVANCE) spectrometer with Cu Kα irradiation (λ = 0.15406 nm) at 40 kV and 30mA to examine the graphitization of the carbon xerogel after carbonization. XPS (Kratos Axis Ultra DLD) was used to determine the oxidation states of carbon xerogels. A monochromatic AlKa was used as an X-ray source (anode HT = 15 kV). The residual pressure in the ion-pumped analysis chamber was lower than 5 $x10^{-7}$ torr. The binding energies were referenced to the O1s peak (529.2 eV) to account for the effects of charging. Raman spectra were recorded with a Senterra Dispersive Raman Microscope (Bruker Optics) using laser excitation wavelength at 532 nm with a TE-Cooled CCD detector. The electrical conductivity values of the carbon xerogels were obtained by a custom-buit two-point probe. A conductivity meter (Keithley 6517A) was connected to the probe and the current was measured in response to the applied voltage. The sample was compressed in the circular disk form with a diameter of 1.30 cm. The electrical conductivity of the samples was calculated using equation

$$\sigma = I/KVt$$

Where I is the measured current (A), V is the applied voltage (V), t is the sample thickness (cm) and K is the geometric correction factor which is equal to the ratio w/l, where w and l are the probe width and length, respectively (2.15×10^{-3}).

4.3.3 Methodology

4.3.3.1 Synthesis of Polybenzoxazine Xerogels

Sol-gel synthesis method was used to synthesized polybenzoxazine which firstly invented by Ishida [9]. Polybenzoxazine precursor (25 %wt) was synthesized by dissolving CTAB (20 %wt) in N,N, -dimethylformamide (DMF) (47.56 g) and stirring continuously until CTAB was dissolved. Phenol (4.7 g) was then added into the mixture followed by adding formaldehyde solution (8.1 g). At the same time MDA solution was prepared by adding MDA (4.72 g) into DMF (5 g) and stirring until MDA was dissolved. The reaction was kept under 10 ^{0}C by using an ice bath. MDA solution was slowly dropped into the mixture followed by continuous stirring for 20 minute at room temperature. The molar ratio of phenol: formaldehyde: MDA was 2: 4: 1. The synthetic reaction was shown in figure 4.1. After that the precursor was transfer to a vial with seal and put into oil bath at 80 ^{0}C for 24 hr. Benzoxazine xerogels were cut into small pieces and then removed CTAB out via soxhlet method and using ethanol as solvent for 24 hr. Removed ethanol from benzoxazine xerogel by drying in the oven at 80 ^{0}C overnight. The benzoxazine was placed in an oven by using the curing step at 110, 140, 150, 160, 170 ^{0}C and kept for 1 hr at each temperature and lastly increased from 170 to 180 ^{0}C for 40 minutes in order to polymerize benzoxazine xerogels which shown in Figure 4.2. After that DSC, TGA, and FT-IR were used to characterize polybenzoxazine xerogels.

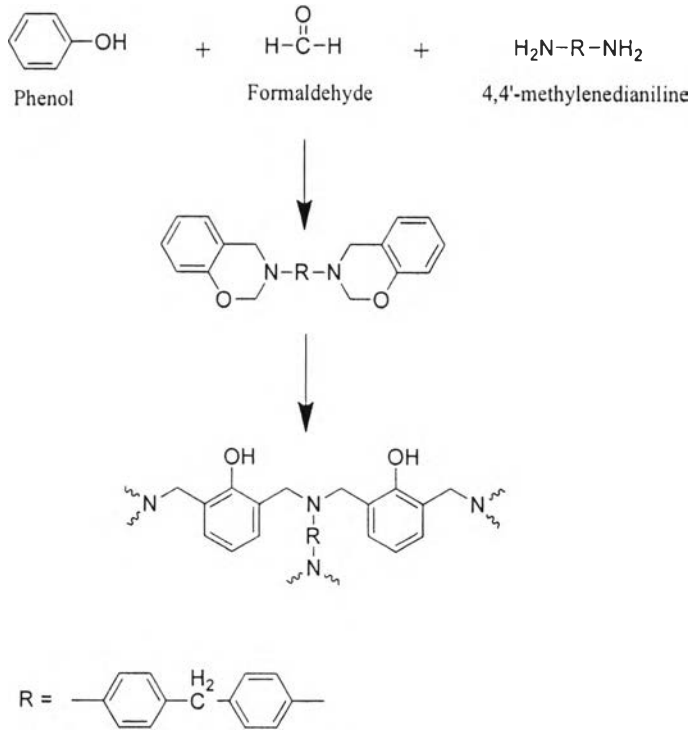

Figure 4.1 Synthesis of methylenedianiline-based polybenzoxazine.

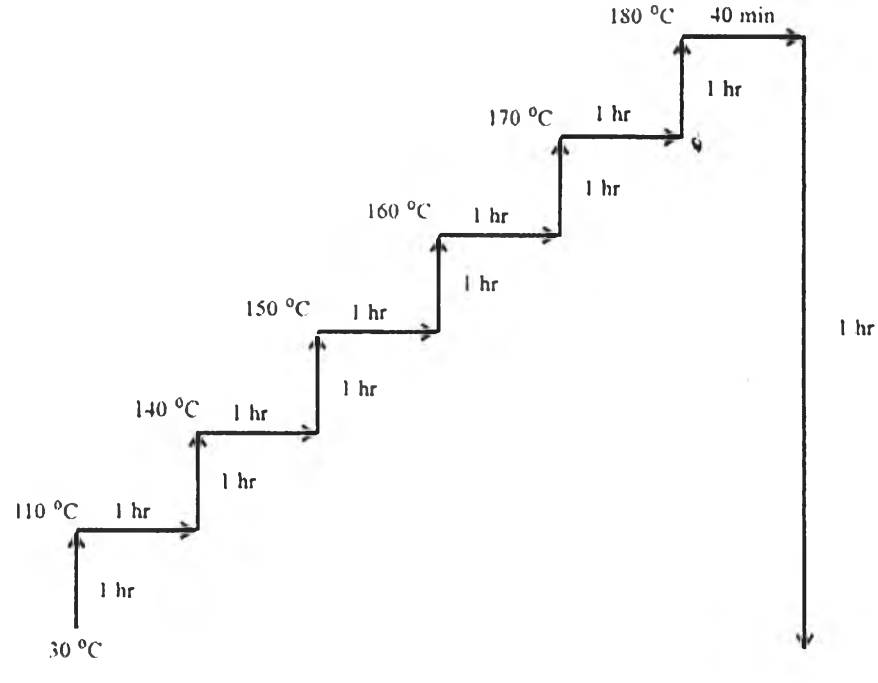

Figure 4.2 Curing step of polybenzoxazines.

4.3.3.2 Preparation of Carbon Xerogels

Pyrolysis temperatures of polybenzoxazine were varied at 800, 900, and 1000 ^{0}C under a condition of nitrogen flow rate at 550 cm^3/ min. The heating profile of each condition was shown on Table 4.1.

After that surface activation was required to improve wettability and surface area of carbon xerogels. Activated carbon xerogels (ACX) were prepared by using the heating profile from room temperature to 900 °C for 3 hr and hold at 900 °C for 3 hr in CO_2 atmosphere.

Table 4.1 The pyrolysis conditions of carbon xerogels

800 °C		**900 °C**		**1000 °C**	
Temperature	**Time**	**Temperature**	**Time**	**Temperature**	**Time**
25-200	2 hr	25-200	2 hr	25-200	2 hr
200-300	2 hr	200-300	2 hr	200-300	2 hr
300	1 hr	300	1 hr	300	1 hr
300-400	3 hr	300-400	3 hr	300-400	3 hr
400	2 hr	400	2 hr	400	2 hr
400-600	2 hr	400-600	2 hr	400-600	2 hr
600-800	2 hr	600-800	2 hr	600-800	2 hr
800	1 hr	800-900	2 hr	800-1000	2 hr
-	-	900	1 hr	1000	3 hr

4.3.3.3 Characterization of Carbon Xerogels

The effect of pyrolysis temperature to the structure of carbon xerogels has been examined. The changing in chemical structure of polybenzoxazine was investigated by FTIR. In addition, TGA and DSC were used to explore thermal properties. Moreover, XRD technique, Raman spectroscopy, and XPS were used to analyze the changing on structure of carbon xerogels. The electrical property of carbon xerogels under various pyrolysis temperature treatments was observed at room temperature by an electrometer with two-point probe (Keithley model 6517A).

4.4 Results and Discussions

4.4.1 Preparation of Carbon Precursor Derived from Polybenzoxazine

From the previous, carbon materials that were attractive to use as electrode for supercapacitors were graphene and carbon nanotube due to good at electrical properties and high surface area. But both of them have weak points in terms of industry, which are unacceptable cost and mass production difficulty. For many years that scientists tried to produce graphene by using various methods whether chemical modification or highly pyrolysis temperature (>2500 ^{0}C) which were not worth. To replace previous method and to overcome the limitation, using another carbon precursor and converted to carbon-like graphene structure is interesting. In our work polybenzoxazine was chosen to be organic carbon precursor due to flexibility on structure designed. In order to obtain the resulting carbon with high electrical conductive property, highly aromatic contents precursor was chosen. In Figure 4.3 was shown the chemical structure of benzoxazine precursor and structure of polybenzoxazine after ring opening polymerization.

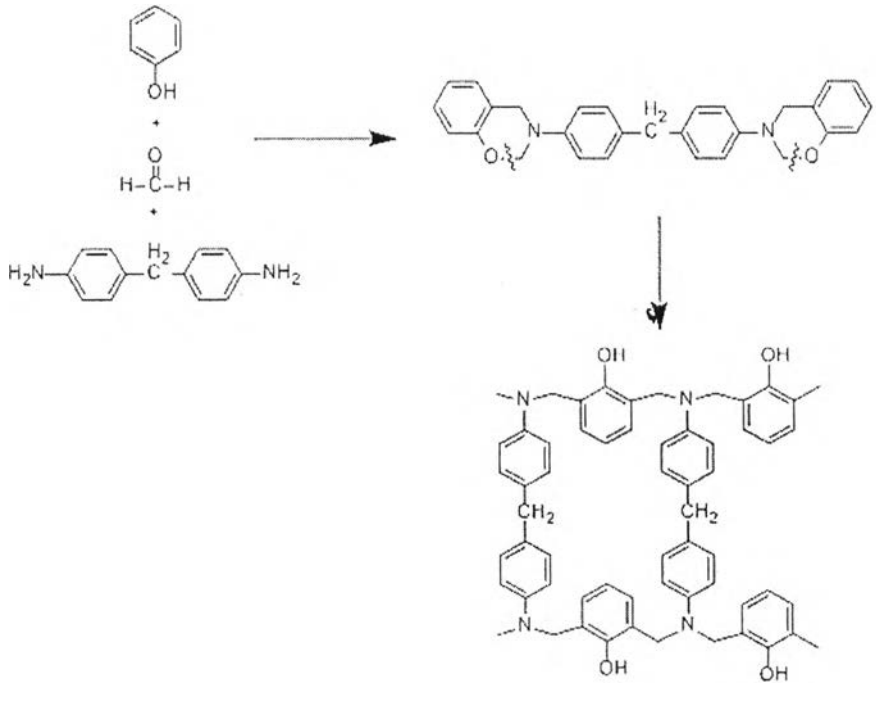

Figure 4.3 Chemical structures of benzoxazine precursors and polybenzoxazine.

FT-IR was used to confirm the chemical structure of polybenzoxazine after the ring opening polymerization as shown in figure 4.4. Benzoxazine precursor shown characteristic absorption band at 805.36 for C-H bending and ring puckering. The absorption bands at 947 and 1225 cm^{-1} were referred to C-O-C stretching of ozaxine ring which will disappear after benzoxazine fully polymerized. C-N stretching displays around 1112-1247 cm^{-1}. C=C stretching of aromatic appears at 1502-1675 cm^{-1} [10]. After polymerization, disappear of C-O-C stretching was observed and O-H broad brand also appear due to ring opening polymerization created free OH group which related to the mechanism of ring opening polymerization as shown in Figure 4.3. Peak at 1518 cm^{-1} represented tri-substituted of benzene ring but after ring opening polymerization this peak shifted to 1660 cm^{-1} because benzene ring was changed to tetra-substituted.

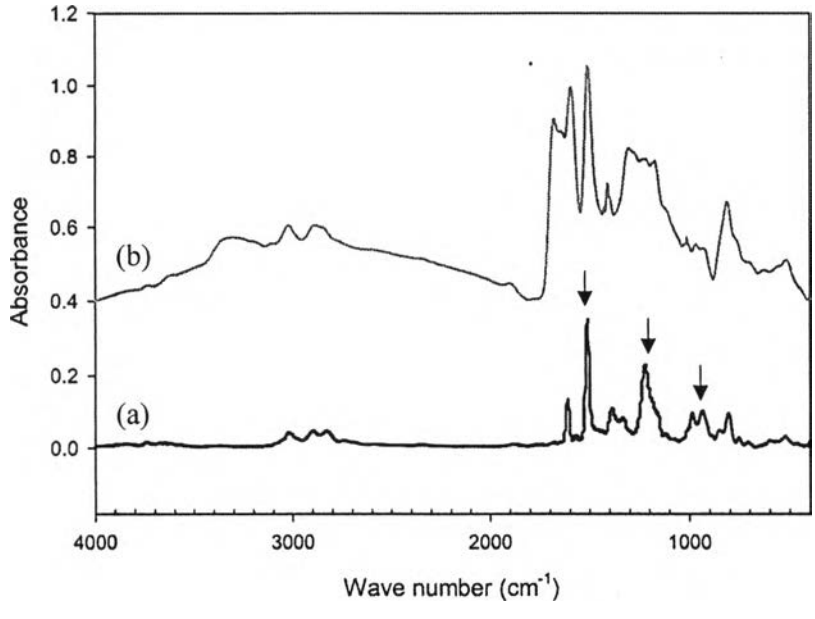

Figure 4.4 FT-IR spectra of (a) benzoxazine precurosr and (b) partially cured of polybenzoxazine.

DSC technique was used to find curing temperature by observing from the exothermic peak. DSC thermograms as shown in figure 4.5 shown exotherm peaks of benzoxazine precursor at 180 °C and 264 °C which represent the ring opening polymerization of ozaxine ring, after benzoxazine precursor was cured,

exotherm peak at 180 °C was disappeared but exotherm peak at 264 °C still remained just decreasing of area under peak. The results indicated that ring opening polymerization of benzoxazine precursor was partially occured. The maximum temperature that was used to cure benzoxazine precursor was 180 °C because benzoxazine xerogels had very dense and rigid structure lead to difficulty for dissipating heat through the bulk of sample. In order to distribute heat across the bulk sample, slow heating rate in curing step was required. Moreover, benzoxazine precursor was very sensitive to thermal if curing temperature raised to higher than 180 °C, polybenzoxazine xerogels were burnt and morphology at the surface of polybenzoxazine xerogels were damaged and collapsed. So as the result

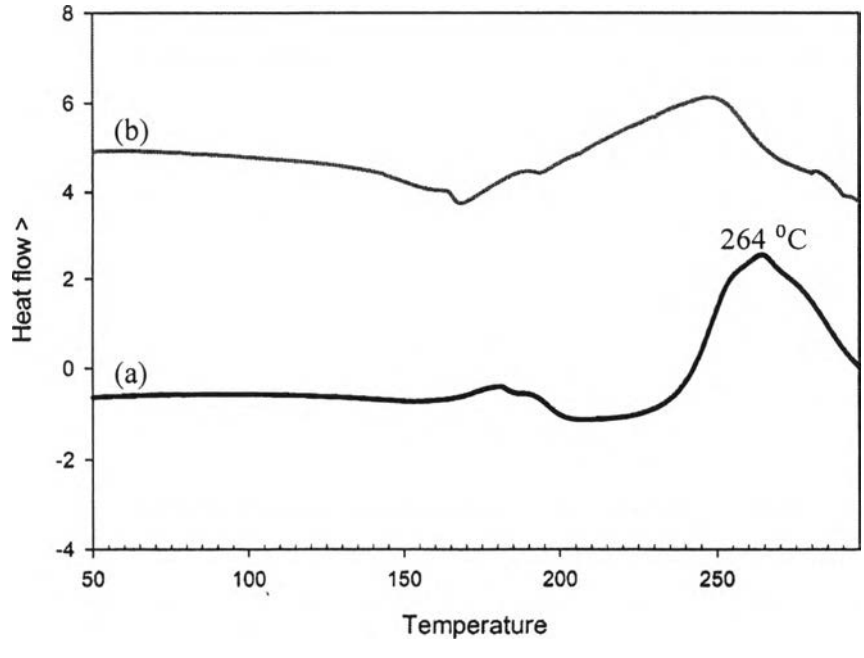

Figure 4.5 DSC thermogram of (a) benzoxazine precursor and (b) partially cured of polybenzoxazine.

The SEM micrographs of polybenzoxazine xerogel (non-surfactant) and polybenzoxazine xerogels (20 %wt CTAB) were shown in figure 4.6. From benzoxazine precursor structure which composed of highly aromatic structure affected to dense sol-gel formation as shown in figure 4.6 (a). Not only the effect

from chemical structure of benzoxazine precursor but phase separation process during the 3D interconnected sol-gel formation also had an influence on the structure of polybenzoxazine xerogels. The parameter that impinged upon phased separation process was the difference between solubility parameters of benzoxazine and solvent. If solubility of benzoxazine was very close to that of solvent, the phase separation process will take long time to occur, providing very dense structure [11]. In this study, DMF was used as a solvent which has solubility parameter close to benzoxazine because from the observation, the phase separation took place rather slowly (about 3 hr) causing the sol-gel aggregration. In order to expand the structure of polybenzoxazine xerogel, the surfactant (CTAB) was then used. It was obvious that CTAB can perform well in this system, forming micelles which turned hydrophobic (tail) inside and turned hydrophilic (head) outside. Benzoxazine which was hydrophobic would permeate into the micelles. Finally, the connected particles of benzoxazine were formed in spherical shape and after solvent removal, 3D interconnected network was obtained. Another role of CTAB was to make the sol-gel structure less pack. From the SEM micrograph, the different between sol-gel structure of polybenzoxazine before and after adding surfactant was clearly seen. In figure 4.6 (b), round particles with less dense structure were formed. On the other hand, polybenzoxazine xerogels without adding of CTAB showed polybenzoxazine particles connected like coral.

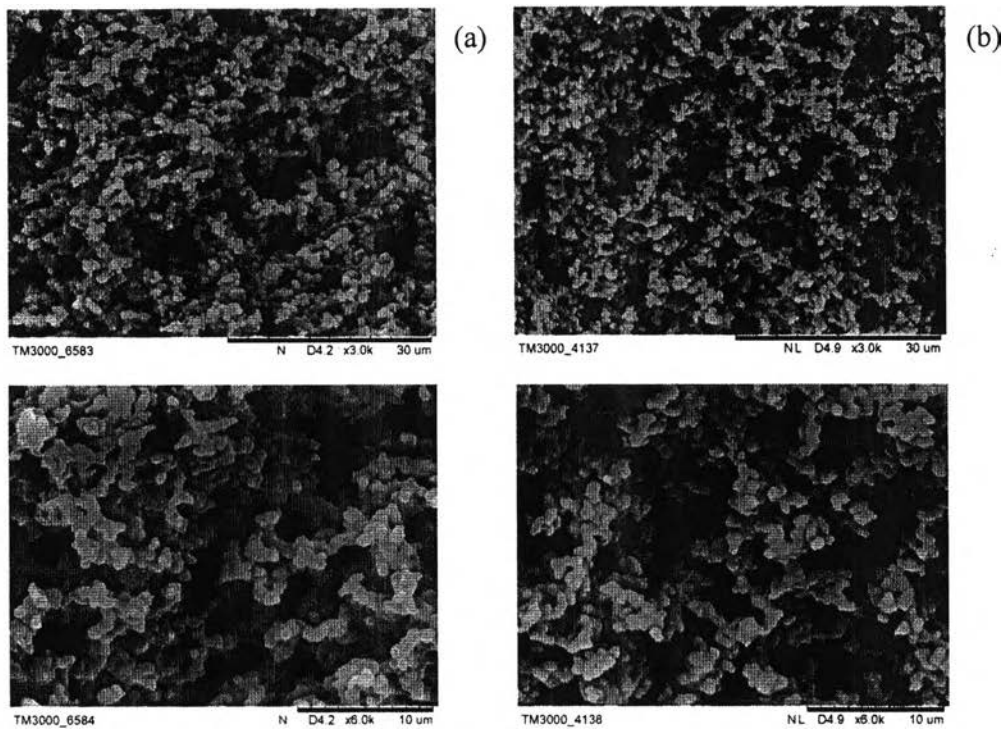

Figure 4.6 Polybenzoxazine xerogels without surfactant (a), Polybenzoxazine xerogels with surfactant (b) (up) low magnification, (down) high magnification.

4.4.2 Preparation of Carbon Xerogels

Pyrolysis process was the way to convert polybenzoxazine xerogels to carbon. Transformation of polybenzoxazine xerogels (carbon precursor) to carbon was occurred through pyrolysis under inert atmosphere with slow heating rate. During the process, polybenzoxazine started to decompose and eliminate small organic molecules (volatile materials) as shown in TGA thermogram in figure 4.7. As can be seen from the results of TG-DTA, polybenzoxazine xerogels started to decompose at 240 ^{o}C and provide high char yield about 32% according to high aromatic content of polybenzoxazine lead to exhibit high thermal stability and high thermal resistance from the very rigid strucuture. Compare to senior work, khiatdet and coworker used the same benzoxazine precursor but synthesized via bulk polymerization. They obtained higher amount of char yield (46%) that contrasted to the report form Lorjai [12]. In that case, they compared thermal stability between

bulk polybenzoxazines and polybenzoxazine aerogels. Bisphenol-A and aniline were used as precursor. The char yield from bisphenol-A/aniline based polybenzoxazine aerogel increased up to 24% and 97% higher than the bulk due to continuous micropores within the aerogel structure introduce elevation of the residence time of the primary decomposition products to form secondary and heterocyclic compounds [13]. The result from Lorjai [13] could not be used to discuss amount of char yield in our work because using different benzoxazine precursors. In this studied, polybenzoxazine had very stiff and rigid structure due to aromatic compounds made them generated highly dense structure. During the decomposition process, small molecules and volatile materials could not go out easily but better than bulk polybenzoxazine from Khiadet because porous structure of xerogels had more free space to allow small molecules to reach out and causing to less char yield [12].

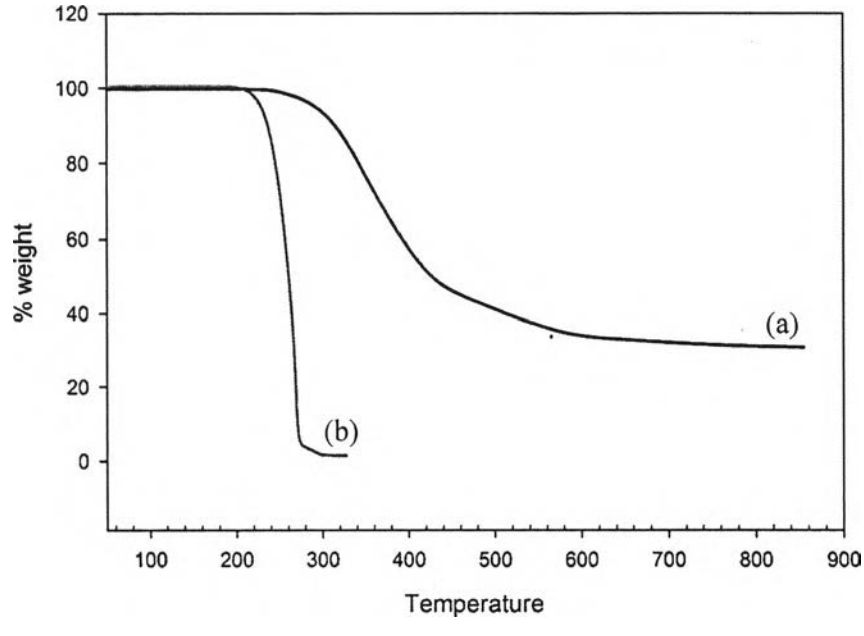

Figure 4.7 TGA thermogram of (a) polybenzoxazine and (b) CTAB .

Moreover, TGA was used to characterize the amount of char yield of CTAB in order to confirm the total char that was left after pyrolysis not came from CTAB because CTAB show zero char yield as shown in TGA thermogram.

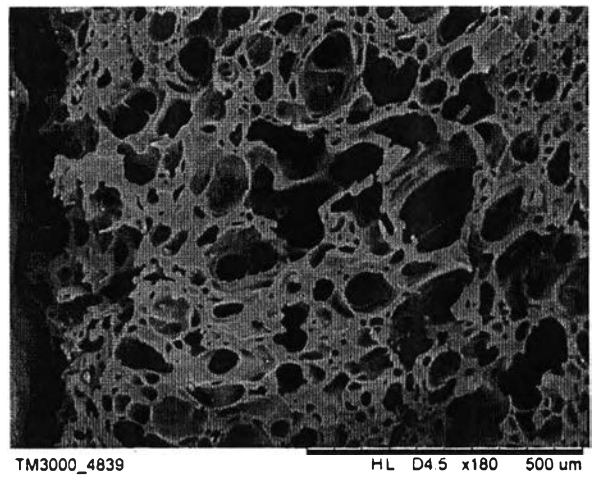

Figure 4.8 SEM micrograph of carbon xerogels.

Morphology of carbon xerogels after passing carbonization process was shown in figure 4.8. From previous discussion about structure of polybenzoxazine xerogels (carbon precursor) that were added surfactant in order to expand the structure of polybenzoxazine sol-gel, after pyrolysis polybenzoxazine particles fused together and forming thin carbon layer.

4.4.3 Effect of Pyrolysis Temperature to Changing Structure of Carbon Xerogels

The main factor that defines the properties of carbon was chemical structure of carbon rich organic precursors, in this study was polybenzoxazine. In the process of pyrolysis, polybenzoxazine went through the thermal decomposition, which eliminated volatile materials. With increasing of pyrolysis temperatures, condensation reaction was originated and localized graphitic units commence to grow and aligned into graphite like [14]. Partially cured of polybenzoxazine xerogels provided more advantages than fully cured of polybenzoxazine xerogels. Because partially cured polybenzoxazine xerogels was the mixture of two phases, one was the rigid phase and the second one was the flexible phase. The flexible phase can be changed to fluid state during the pyrolysis process which led aromatic molecules to align with each other and converted into highly ordered graphite. On the other hand,

the rigid phase remained a solid phased during carbonization and that limited mobility of crystallites so rigid amorphous which composed of randomly-oriented graphene layer was formed. During the pyrolysis process, aromatic molecules inside carbon precursors aligned with each other and formed extensive pre-graphitic structure. After underwent higher temperature treatment, carbon xerogels can be converted into highly ordered graphite [1]. In this study, carbon precursor has high aromatic content and rigid structure, the aromatic molecules inside the structure had more chance to convert into highly ordered. In order to increase mobility of the carbon structure, the sol-gel synthesis method was used to prepare the carbon instead of bulk synthesis to yield looser benzoxazine sol-gel structure which increased free space for aromatic molecules to rearrange into highly ordered structure.

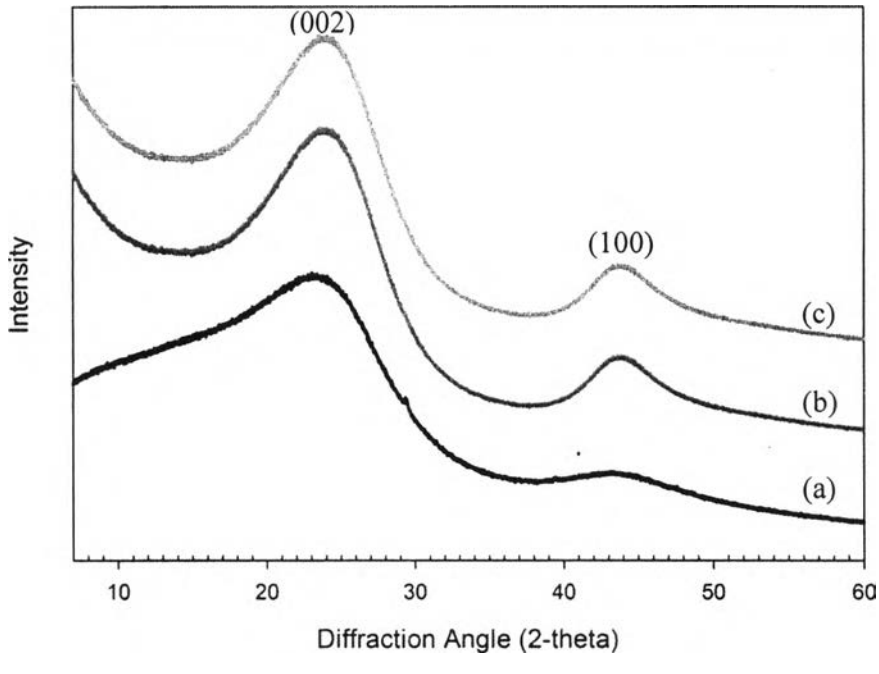

Figure 4.9 X-ray diffractograms of carbon xerogels (CX) at different pyrolysis temperatures (a) 800, (b) 900, and (c) 1000 ^{o}C.

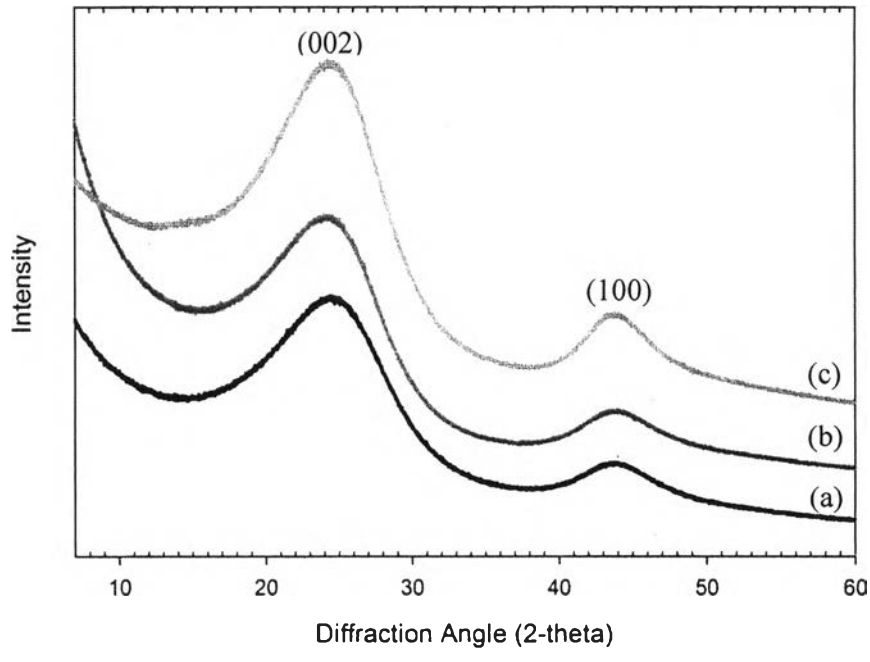

Figure 4.10 X-ray diffractograms of activated carbon xerogels (ACX) at different pyrolysis temperatures (a) 800, (b) 900, and (c) 1000 ^{o}C.

Carbon xerogels (CX) were obtained from pyrolysis of polybenzoxazine under 800, 900, and 1000 ^{o}C in inert atmosphere. To understand the changing of carbon xerogels structure at different pyrolysis temperatures, XRD technique was used to identify as shown in figure 4.9. It could be seen from the XRD diffractograms that the pattern of carbon xerogels displayed two broad peaks at around 24 and 44^{0} corresponding to (0 0 2) and (1 0 0) in accordance with turbostratic structure [15-16]. The small peak at 44^{0} appears from the ordering of C atoms inside the graphene layer. From now it could be considered graphene layer within the turbostratic structure as individual two-dimensional crystallites built up of hexagonal two-dimensional unit cells and with the in-plane size equal to the layer diameter. The maximum intensity peak which located at 24^{0} exhibited that graphene layers are already formed and organized as parallel layers spaced at a relatively well-defined interplanar distance [17]. Two broad peaks on XRD diffractogram indicated that carbon xerogels were still in amorphous form. Focusing on the pyrolysis temperature, after increasing of pyrolysis temperature, the two peaks became sharpen

and the positions of the two peaks slightly shifted to the higher angles. Moreover, the intensity was increased indicating that the structures of carbon have some rearrangement to higher ordered structure.

After carbon xerogels were activated surface under carbon dioxide atmosphere at 900 °C, the changing of XRD diffractogram was shown in figure 4.10. It was obvious that intensity of XRD diffractograms was increased and sharpens because the activation process occurred at high temperature causing the molecules inside the structure relaxed and rearranged into higher order structure. After calculated the average crystallite height (L_c) which can be calculated from Scherrer formular, where λ is 0.15406 nm, θ is the bragg angle, and β is the full width at half maximum [18]. The results of crystallite height of CX and ACX as shown in table 4.2, when pyrolysis at higher temperature the crystallite height was decreased due to higher temperature the aromatic molecules obtained higher energy to form, pack and rearrange the structure to higher order crystal which matched to the resulted from XRD. In addition, the results from calculating crystallite height of carbon xerogels after the activation process shown that L_c decrease. Because activated carbon surface with CO_2 was the etching process. When surface of carbon was etched, crystallites thickness also decreased comparing to carbon xerogel. As the results of crystallite thickness as shown on table 4.2, ACX 1000 has less crystal thickness layer around 0.88 nm.

$$L_c = \frac{0.89\lambda}{(\beta_{002} \times cos\theta_{002})}$$

Table 4.2 Crystalline parameters of CX and ACX at various pyrolysis temperature from XRD

Sample	$2\theta_{002}$ (^{0})	$2\theta_{100}$ (^{0})	β_{002} (^{0})	d_{002} (nm)	L_c (nm)
CX 800	23.574	45.60	6.130	3.77	1.31
CX 900	24.510	43.62	7.981	3.63	1.01
CX 1000	24.312	44.04	8.366	3.65	0.96
ACX 800	24.615	44.23	7.464	3.61	1.10
ACX 900	24.350	44.06	8.190	3.65	0.98
ACX 1000	24.680	43.58	9.119	3.60	0.88

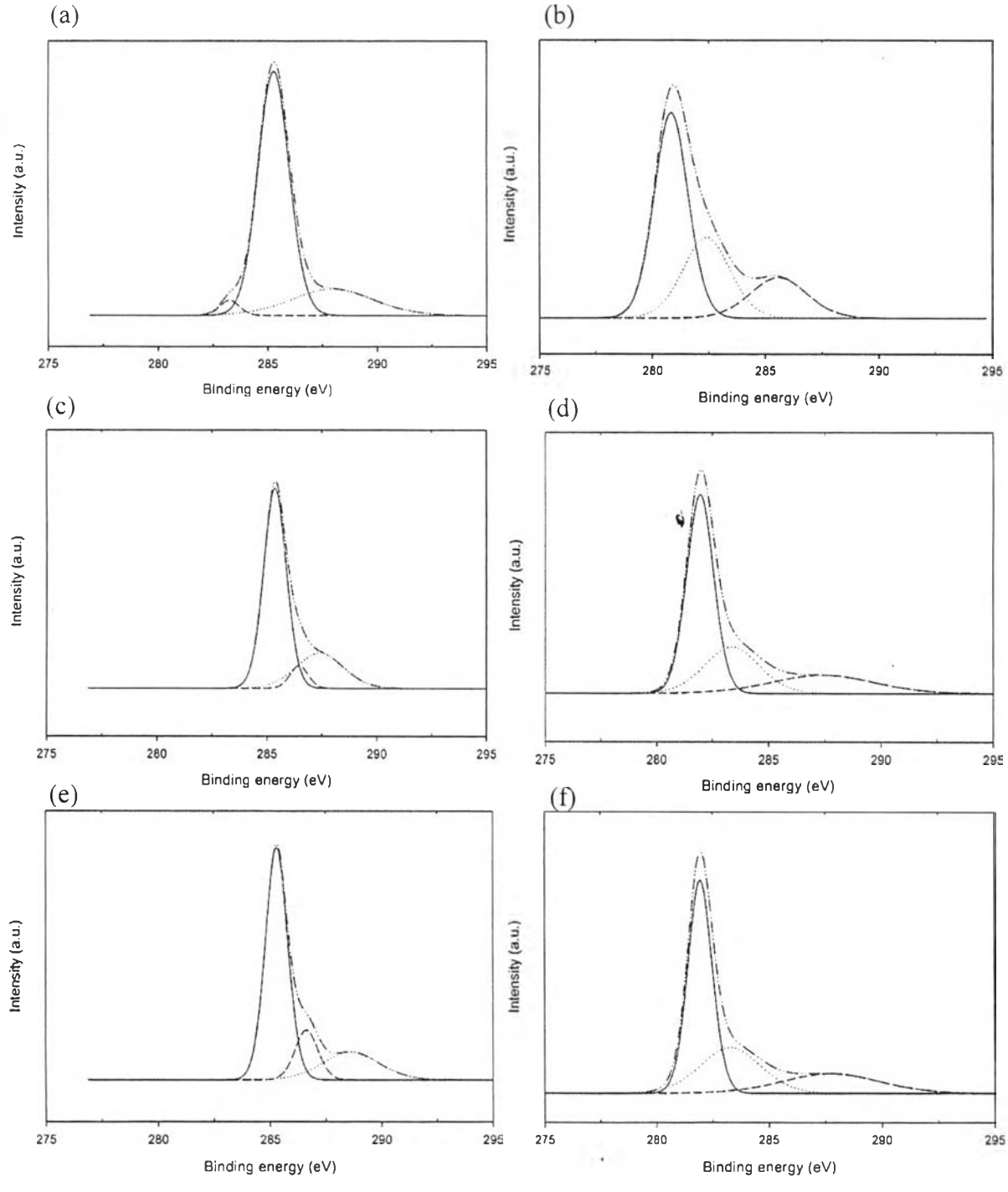

Figure 4.11 High-resolution C 1s XPS spectra carbon xerogels at different pyrolysis temperature; (a) CX 800, (b) ACX 800, (c) CX 900, (d) ACX 900, (e) CX 1000, (f) ACX 1000.

Table 4.3 XPS Data of C1s of CX and ACX at various pyrolysis temperatures

Sample	C-C	C-O	O-C=O
CX 800	285.255	283.262	287.947
CX 900	285.352	286.479	287.411
CX 1000	285.297	286.625	288.647
ACX 800	280.847	282.407	285.589
ACX 900	281.926	283.353	287.415
ACX 1000	281.948	283.309	287.740

High-resolution C 1s XPS spectra are shown in figure 4.11 and Table 4.3 also providing an analysis of the spectrum peaks which was the most probable origin of the peaks with their binding energies of each groups. For CX at higher pyrolysis temperature, the peaks positions were shifted to higher binding energy. The spectra at 285 eV indicating the C-C sp^2 bonds of each sample did not change at each temperature. The spectra of carboxylate C atoms (O-C=O) when increasing of pyrolysis temperature slightly changed from 287 eV to 288 eV. The position of spectra of C atoms in C-O bonds representing carbon bonds with sp^3 hybridization was obviously shifted to higher binding energy (283 eV to 286 eV). Moreover, the relative content also increased from 3% to 14.4%. Because as increasing of pyrolysis temperature, carbon atoms absorbed energy which high enough to break $\prod$ bond between O-C=O of carboxylate. The XPS spectra of CX 1000 were mostly fitted to XPS spectra of graphene which appearing at 284.8 eV, 286.3 eV, and 288.9 eV [19].

After the surface activation process, the peak positions of binding energies were obvious shifted to lower binding energy. Activated surface of carbon xerogels was the process that introduced large amount of oxygen atoms to the surface of carbon xerogels by substituted carbon with oxygen atom into the main chain as related to the result of the molar ratio between C/O as shown in table 4.4 and the result from XPS. As the results, after the activation process, the molar ratio of C/H were increased which means that H atom was removed from the carbon xerogels surface. In addition, the molar ration of C/O also decreased indicated that amount of

oxygen increased on the surface. When oxygen intruded in carbon main chains it caused the reduction of covalence bonding between C-C that lead to decreasing of binding energy of C-C and C-O [3]. Moreover, when oxygen introduced into the main chain of carbon it increased the flexibility of carbon main chain which causing the reduction of binding energy as seen from the results of XPS spectra that position peaks of ACX were shifted to lower binding energy. The position that oxygen atoms substituted into the carbon surface was shown in figure (1) 4.12 rather than position (2) because from the XPS spectra, the peak position of O-C=O did not change which implied that oxygen atoms did not substitute in the position (2) as shown in figure 4.12.

The lists elemental analysis data of the carbon xerogels and activated carbon xerogels at different pyrolysis temperatures was shown on table 4.2. It can be seen that the content of C element of the CX 1000 was 95.5 wt%, which indicated that pyrolysis polybenzoxazine xerogel at 1000 °C was successfully due to the removal of light molecules and gases which generated from the cracking reactions during carbonization process[20]. After activated surface of carbon xerogels with CO_2, all of activated carbon xerogels had higher content of O due to activation process generated oxygen onto the surface of carbons, related to the molar ratio of C/H and C/O.

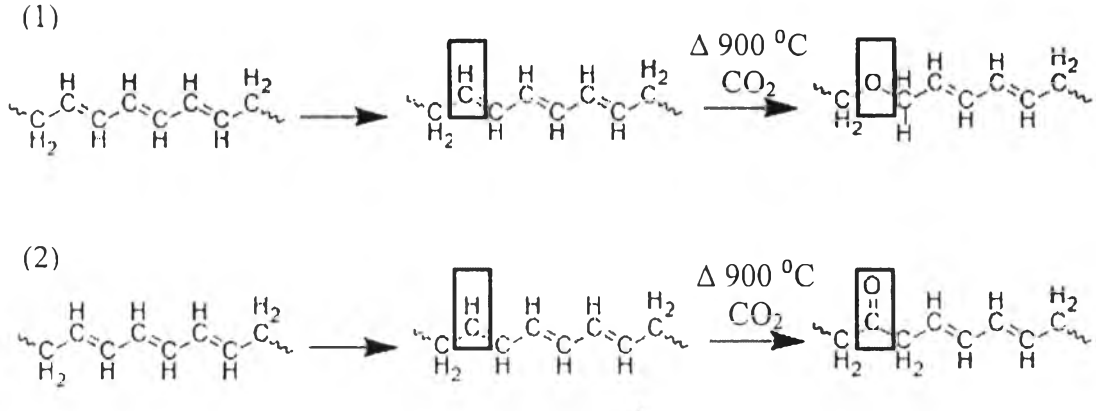

Figure 4.12 The position of oxygen substitution to the carbon xerogels surface.

Table 4.4 The chemical composition and molar ratio of C/H and C/O of CX and ACX under various pyrolysis temperature

	Chemical compositions				Mol ratio	
Sample	**Nitrogen (wt%)**	**Carbon (wt%)**	**Hydrogen (wt%)**	**Oxygen (wt%)**	**C/H**	**C/O**
CX 800	8.7250	88.0	2.310	0.9650	3.173	122.167
CX 900	6.9248	91.4	0.899	0.7762	8.473	157.051
CX 1000	3.8453	95.5	0.353	0.3017	22.544	421.060
ACX 800	5.7322	90.5	0.558	1.3912	13.516	86.690
ACX 900	6.8212	91.0	0.672	1.5068	11.28	80.499
ACX 1000	3.7853	95.3	0.407	0.5077	19.514	250.54

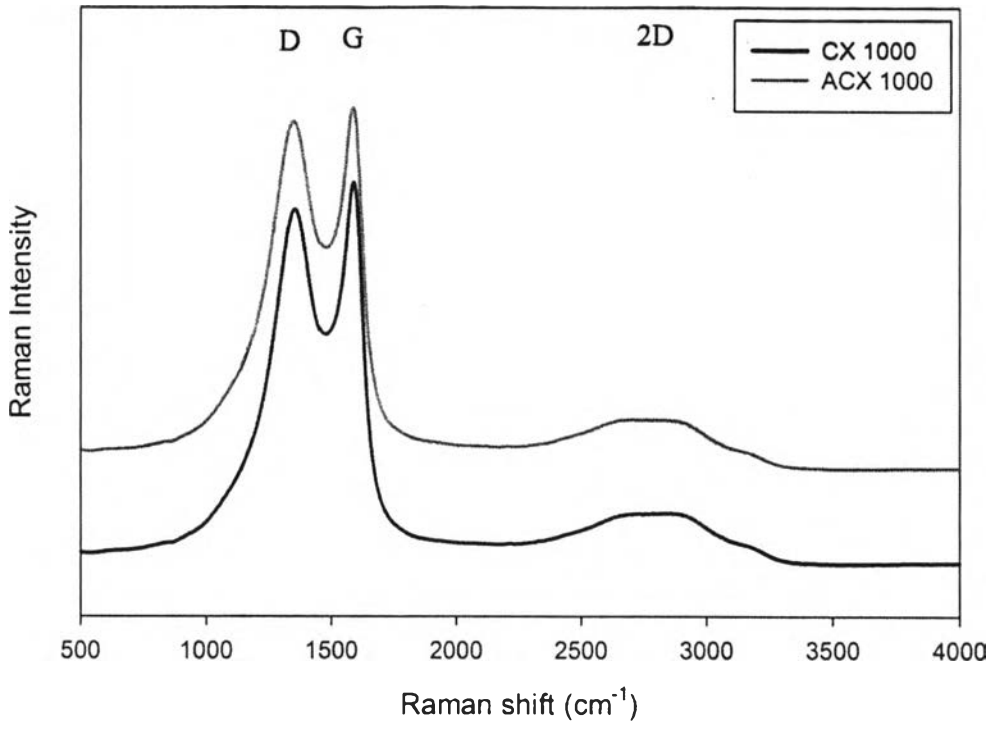

Figure 4.13 Raman spectra (excitation at 532 nm) of CX (1000) and ACX (1000).

As the results from previously, pyrolysis carbon xeroges at 1000 °C was the most effective temperature because provided carbon structure which closed to graphene-like structure as can be seen form the results of XRD and XPS. So to obtain more details about carbon structure, Raman spectroscopy was used to investigate CX 1000 and ACX 1000. Raman characterization as shown in figure 4.13, CX 1000 appeared the G band which represented the planar configuration sp^2 bonded carbon that constituted graphene at 1586.36 cm^{-1}, while the D band corresponds to the disorder band or the defect band which represents a ring breathing mode for sp^2 carbon rings appear at 1351.35 cm^{-1}. It is demonstrated that the intensity ratio (I_D/I_G) of D band and G band of CX 1000 was 0.93, implying that CX 1000 contained graphitic crystalline structure [21]. But consideration only G band and D band was not enough to confirm that CX 1000 had graphene like structure. The 2D band or G'-band were also regarded to determine the different between graphite and graphene. The 2D band appeared low hill at 2785.66 cm^{-1} which indicated that CX 1000 had some part of structure that started to transform to graphene-like structure but it was still in amorphous form, the layer thickness was still high and had more than one component [22-23]. After activated carbon xerogels surface (ACX 1000), the position of D and 2D band were a little bit changed by the following; D =1346.55 cm^{-1}, 2D = 2766.69 cm^{-1}. When the 2D band of ACX 1000 shifted to lower wave number it implied that the layer thickness of graphene-like structure decreased. Intensity ratio (I_D/I_G) of ACX 1000 equal to 0.96 and CX 1000 equal to 0.93 which was slightly increase after surface activation. The intensity ratio of D band and G band (I_D/I_G) was measure the degree of disorder and implied the graphitic crystalline structure of carbon. From raman spectra, the intensity ratio (I_D/I_G) of ACX 1000 was higher than CX 1000 due to activation process created the defect on carbon surface. But activation process provided advantage by reducing layer thickness of graphene-like carbon. Cancado and coworker proposed the general equation to determine the crystallite size (L_a) by following this equation

$$L_a = (2.4 \times 10^{-10})\lambda_l^4 (\frac{I_D}{I_G})^{-1}$$

Where λ_l was the laser line wavelength in nanometer units [24], as the results from calculating follow this equation, CX 1000 shown L_a = 20.671 nm and ACX = 20.025

nm. It was obvious that crystallite size decreased because in the activation process which gradually introduced thermal to the crystallites, on the other word was called annealing process. At that time, the stress that left inside the crystallites part can be relaxed. But when the temperature was cooled down to the room temperature, the new stress appeared due to local inhomogeneities and caused to shrinkage of crystallites lead to the presence of unavoidable intercrystalline porosity [25].

From the results of XRD, XPS, and Raman spectra, we can confirm that synthesized carbon xerogels had transformation to graphene-like carbon structure, and still in amorphous form when increasing of pyrolysis temperature. Graphene-like carbon xerogel was obtained after pyrolysis at 1000 ^{o}C with very slow heating rate. In generally, carbon was hydrophobic which is difficult to disperse due to aggromeration. To prevent the problem from agglomeration of carbon surface treatment was required to improve wettability by using surface activation process.

4.4.4 Electrical Conductivity of Carbon Xerogels

The electrical conductivity of carbon xerogels and activated carbon xerogels at different pyrolysis temperature was shown on table 4.5. Carbon xerogels which pyrolyzed at 1000 ^{o}C (CX 1000) provided the highest conductivity. When temperature was increased, that vibration energy was also increased and created more chance for molecules in the carbon structure to localize and rearrange into highly ordered structure.

The resulting carbon provided electrical conductivity higher than senior work about 3 times. Compare to senior work, they used the same type of polybenzoxazine carbon precursor but synthesized in different way which was bulk polymerization [12]. Synthesized via bulk polymerization provided very dense and rigid structure (also called hard carbon) and when it was fully cross-link, the mobility was greatly restricted and prohibited graphitization process causing to formation of rigid amorphous structure that composed of randomly-oriented graphene layers [24]. The maximum of conductivity that they obtained was 3800 S/cm when pyrolysis at 1200 ^{o}C. On the other hand, carbon xerogels which synthesized via sol-gel process provided looser structure in form of porous carbon and as we mention before that

polybenzoxazine was not fully crosslink so the final carbon xerogels was the mixture of soft carbon and hard carbon. Due to looser structure of polybenzoxazine which means that it had more free space for aromatic molecules to align themselves to from highly order structure during pyrolysis process. From the polybenzoxazines structure that presence of unsaturated molecules (aromatic molecules) which caused the reducing of the gap between ground state and excited state of the electronic band and this gap will be more decreased when heat treatment temperature was increased. The decreasing of this gap reduced the resistance of carbons [25]. In addition, the result of graphene-like carbon structure from heat treatment at higher, also increased proportion of conjugated carbon in the sp^2 state as shown in the results from XRD and raman spectra. When conjugated carbon was increased, the conductivity also increased due to electrons associated with π-bonds were delocalized and became available as charge carriers [8]. The discussion from the above supported why pyrolysis carbon xerogels at 1000 ^{0}C provided the highest electrical conductivity about 9808.736 S/cm.

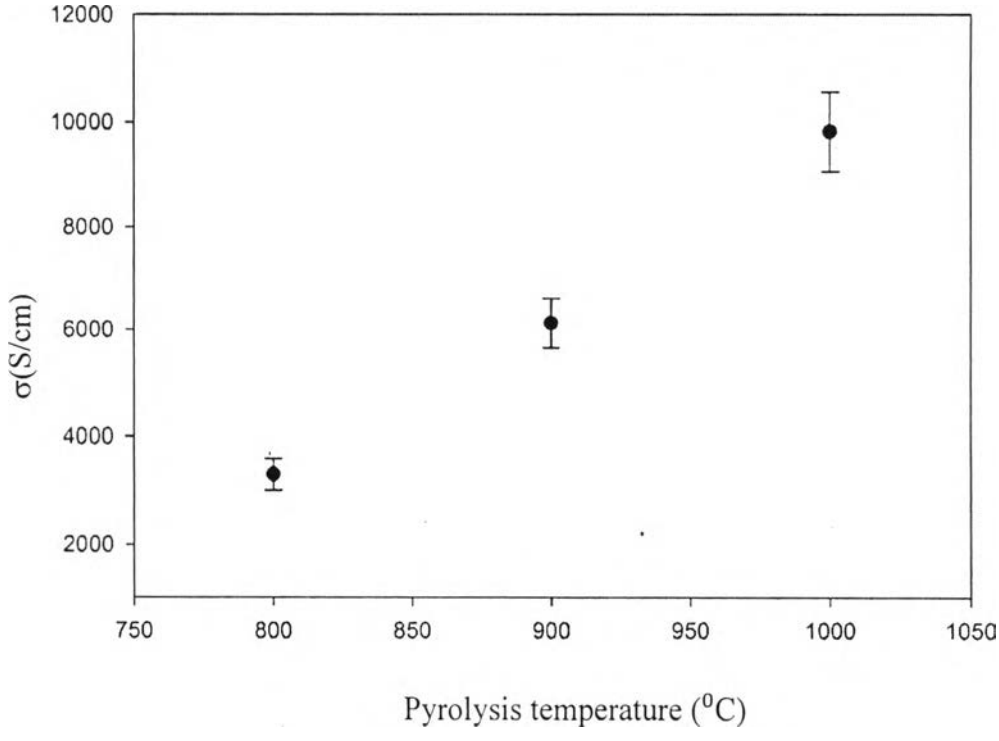

Figure 4.14 The electrical conductivities of carbon xerogels at various pyrolysis temperatures.

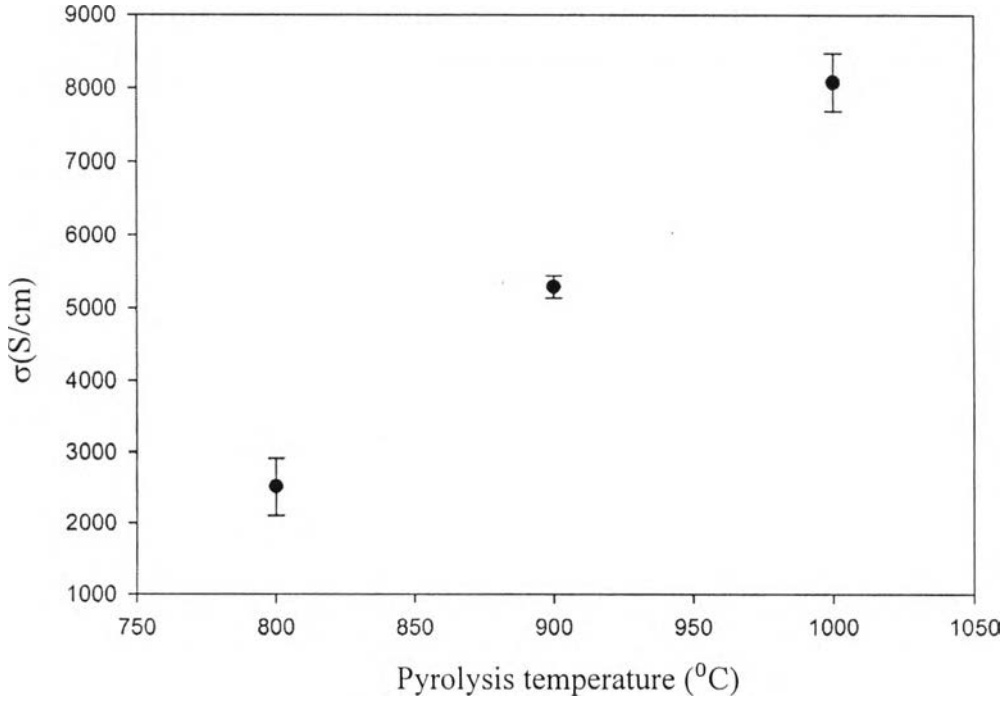

Figure 4.15 The electrical conductivities of activated carbon xerogels at various pyrolysis temperatures.

Table 4.5 The electrical conductivities of carbon xerogels and activated carbon xerogels

Pyrolysis temperature	Conductivity, σ (S/cm)	
	Carbon xerogels (CX)	Activated carbon xerogels (ACX)
800 °C	3299.203	2507.97
900 °C	6121.337	5287.34
1000 °C	9808.736	8077.65

Comparing the electrical conductivity between carbon xerogels at various pyrolyzed temperature was shown in Figure 4.14 and activated carbon xerogesl as shown in figure 4.15, it was obvious that after surface activation under CO_2 atmosphere at 900 °C, conductivity of ACX was decreased because crystallite size decreased as shown form the result of raman spectra. When crystallite size decreased, lead to the increasing of grain boundaries size [26]. These grain boundaries obstructed electrical transport and lead to prominent weak localization caused to decrease of electrical properties [27]. Moreover, activation process introduced oxygen atoms to the surface of carbon xerogels and this also obstructed the transport of electron lead to increasing of resistivity.

4.5 Conclusion

Highly conductive carbons were successfully preparing by pyrolysis of polybenzoxazine xerogels derived from phenol, formaldehyde and MDA. Benzoxazine precursors were synthesized via sol-gel method and then were partially cured in order to obtain polybenzoxazines xerogels. In addition, CTAB was used as soft template to make sol-gel looser. Pyrolysis temperatures were varied to study the changing of carbon xerogels structure and found that at 1000 °C exhibited graphene-like carbon structure. The electrical conductivity also studied and as the results show that increasing of pyrolysis temperature, electrical conductivity also increased due to

aromatic molecules aligned to order structure and lead to decreasing of band gap between ground state and excited state which improved the electron transport. After surface activation, electrical conductivity decreased due to increasing of grain boundaries size that impeded electron hoping. In addition, oxygen atoms that introduced on the surface of carbon xerogels also interrupted electron delocalized and increased the resistance of carbons.

4.6 Acknowledgememts

The author is grateful for the scholarship and funding of the thesis work provided by The Petroleum and Petrochemical College; and The Center of Excellence for Petroleum, Petrochemicals, and Advanced Materials, Thailand.

4.7 References

[1] Pandolfo, A.G., and Hollenkamp, A.F. (2006) Carbon properties and their role in supercapacitors. Journal of Power Sources, 157(1), 11-27.

[2] Allen, M.J., Tung, V.C., and Kaner, R.B. (2009) Honeycomb Carbon: A Review of Graphene. Chemical Reviews, 110(1), 132-145.

[3] Meng, L.Y, and Park, S.J. (2012) Preparation and Characterization of Reduced Graphene Nanosheets via Pre-exfoliation of Graphite Flakes. Bulletin of the Korean Chemical Society, 33(1), 209-214.

[4] Stankovich, S., Dikin, D.A., Piner, R.D., Kohlhaas, K.A., Kleinhammes, A., Jia, Y., Wu, Y., Nguyen, S.T., and Ruoff, R.S. (2007) Synthesis of graphene-based nanosheets via chemical reduction of exfoliated graphite oxide. Carbon, 45(7), 1558-1565.

[5] Worsley, M.A., Pauzauskie, P.J., Olson, T.Y., Biener, J., Satcher, J.H., and Baumann, T.F. (2010) Synthesis of Graphene Aerogel with High Electrical Conductivity. Journal of the American Chemical Society, 132(40), 14067-14069.

[6] Ghosh, N.N., Kiskan, B., and Yagci, Y. (2007) Polybenzoxazines—New high performance thermosetting resins: Synthesis and properties. Progress in Polymer Science, 32(11), 1344-1391.

[7] Holly, F.W., and Cope, A.C. (1944) Condensation Products of Aldehydes and Ketones with o-Aminobenzyl Alcohol and o-Hydroxybenzylamine. Journal of the American Chemical Society, 66(11), 1875-1879.

[8] Biniak, S., Swiatkovski, A., Pakula, M., and Radovic, L.R. (Eds.). (2002) Chemistry and Physics of Carbon. New York: Marcel Dekker.

[9] Ishida, H. and Allen, D.J. (1996). Physical and mechanical characterization of near-zero shrinkage polybenzoxazines. Journal of Polymer Science Part B: Polymer Physics, 34(6), 1019-1030.

[10] Agag, T. and Takeichi, T. (2003). Synthesis and Characterization of Novel Benzoxazine Monomers Containing Allyl Groups and Their High Performance Thermosets. Macromolecules, 36(16), 6010-6017.

[11] Thubsuang, U., Ishida, H., Wongkasemjit, S., and Chaisuwan, T. (2014) Self-formation of 3D interconnected macroporous carbon xerogels derived from polybenzoxazine by selective solvent during the sol–gel process. Journal of Materials Science, 49(14), 4946-4961.

[12] Khiatdet W. (2013) The petroleum and petrochemical college thesis. Preparation of Polybenzoxazine-Derived Partially Ordered Carbon. M.S. Thesis, The Petroleum and Petrochemical College, Chulalongkorn University, Bangkok, Thailand.

[13] Lorjai, P., Wongkasemjit, S., Chaisuwan, T., and Jamieson, A.M. (2011) Significant enhancement of thermal stability in the non-oxidative thermal degradation of bisphenol-A/aniline based polybenzoxazine aerogel. Polymer Degradation and Stability, 96(4), 708-718.

[14] Blanco, C., Bermejo, J., Marsh, H., and Menendez, R. (1997) Chemical and physical properties of carbon as related to brake performance. Wear, 213(1–2), 1-12.

[15] Lin, Q., Tang, H., Guo, D., and Zheng, M. (2010) Preparation and properties of carbon microbeads by pyrolysis of N-phenyl maleimide modified novolac resin. Journal of Analytical and Applied Pyrolysis, 87(2), 276-281.

[16] Lin, Q., Dong, S., Qu, L., Fang, C., and Luo, K. (2014) Preparation and properties of carbon foam by direct pyrolysis of ally novolak-modified bismaleimide resin. Journal of Analytical and Applied Pyrolysis, 106(0), 164-170.

[17] Morjan, I., Voicu, I., Dumitrache, F., Sandu, I., Soare, I., Alexandrescu, R., Vasile, E., Pasuk, I., Brydson, R.M.D., Daniels, H., and Rand, B. (2003) Carbon nanopowders from the continuous-wave CO2 laser-induced pyrolysis of ethylene. Carbon, 41(15), 2913-2921.

[18] Chen, G., Weng, W., Wu, D., Wu, C., Lu, J., Wang, P., and Chen, X. (2004) Preparation and characterization of graphite nanosheets from ultrasonic powdering technique. Carbon, 42(4), 753-759.

[19] Wu, Y., Wang, B., Ma, Y., Huang, Y., Li, N., Zhang, F., and Chen, Y. (2010) Efficient and large-scale synthesis of few-layered graphene using an arc-discharge method and conductivity studies of the resulting films. Nano Research, 3(9), 661-669.

[20] Lu, Q.F., He, Z.W., Zhang, J.Y., and Lin, Q. (2011) Preparation and properties of nitrogen-containing hollow carbon nanospheres by pyrolysis of polyaniline-lignosulfonate composites. Journal of Analytical and Applied Pyrolysis, 92(1), 152-157.

[21] Fan, Z., Yan, J., Zhi, L., Zhang, Q., Wei, T., Feng, J., Zhang, M., Qian, W., and Wei, F. (2010) A Three-Dimensional Carbon Nanotube/Graphene Sandwich and Its Application as Electrode in Supercapacitors. Advanced Materials, 22(33), 3723-3728.

[22] Hodkiewicz, J. (2010a) Characterizing carbon Materials with Raman Spectroscopy.

[23] Hodkiewicz, J. (2010b) Characterizing Graphene with Raman Spectroscopy.

[24] Cançado, L.G., Takai, K., Enoki, T., Endo, M., Kim, Y.A., Mizusaki, H., Jorio, A., Coelho, L.N., Magalhães-Paniago, R., and Pimenta, M.A. (2006) General equation for the determination of the crystallite size La of nanographite by Raman spectroscopy. Applied Physics Letters, 88(16), 163106.

[25] Mrozowski, S. (1979). Specific heat anomalies and spin-spin interactions in carbons: A review. Journal of Low Temperature Physics, 35(3-4), 231-298.

[26] Lopez Maldonado, K.L., de la Presa, P., de la Rubia, M.A., Crespo, P., de Frutos, J., Hernando, A., Matutes Aquino, J.A., and Elizalde Galindo, J.T. (2014) Effects of grain boundary width and crystallite size on conductivity and magnetic properties of magnetite nanoparticles. Journal of Nanoparticle Research, 16(7), 1-12.

[27] Yu, Q., Jauregui, L.A., Wu, W., Colby, R., Tian, J., Su, Z., Cao, H., Liu, Z., Pandey, D., Wei, D., Chung, T.F., Peng, P., Guisinger, N.P., Stach, E.A., Bao, J., Pei, S.-S., and Chen, Y.P. (2011) Control and characterization of individual grains and grain boundaries in graphene grown by chemical vapour deposition. Nat Mater, 10(6), 443-449.